PbSe quantum dot based luminescent solar concentrators

Dennis L. Waldron[1], Amanda Preske[2], Joseph M. Zawodny[3], Todd D. Krauss[2], and Mool C. Gupta[1]

[1] Department of Electrical and Computer Engineering, University of Virginia, Charlottesville, VA 22904

[2] Department of Chemistry, University of Rochester, Rochester, NY 14627

[3] NASA Langley Research Center, Hampton, VA 23666

E-mail: mgupta@virginia.edu

Abstract.

The results are presented for luminescent solar concentrators (LSCs) fabricated with poly(lauryl methacrylate-co-ethylene glycol dimethacrylate) (P(LMA-co-EGDMA)) and Angstrom Bond, Inc. AB9093 acrylic epoxy matrix, high quantum yield (> 70%) PbSe quantum dots (QDs) and silicon photovoltaic (Si PV) cells. LSCs were tested under a lamp with broadband illumination, photon flux-matched to a standard solar spectrum and verified under a calibrated solar lamp source. The P(LMA-co-EGDMA) sample demonstrated the highest power conversion efficiency of any known LSC fabricated with either QDs or Si PV cells, 4.74%. Additionally, increased temperature was shown to reduce efficiency.

Keywords: Quantum dots, lead selenide, PbSe, nanocomposites, optical properties, fluorescence, solar energy, luminescent solar concentrator

1. Introduction

Luminescent solar concentrators (LSCs) are waveguides containing a fluorescent material to capture and guide light to photovoltaic (PV) cells. Compared to a competing technology like geometric solar concentrators, they require no expensive solar tracking mechanisms, reduce PV cell heating, and can absorb both direct and diffuse light. They have been an active area of research since they were first proposed in the late 1970's [1, 2]. Research for a time focused on luminescent dyes, culminating in a power conversion efficiency (PCE) of 7.1% at a geometric gain of 2.5 using two dyes in an acrylic matrix and GaAs cells [3]. A similar system using Si cells and different dyes was able to achieve 4.2% [4].

While most LSCs are planar or planar stacks like the original proposed designs, there have been many attempts at optimizing the architecture for greater PCE. By adding an edge filter to the top surface, for example, up to 20% more current can be realized from the LSC system [5]. Getting away from the traditional paradigm of edge-mounted solar cells,

the price per Watt was able to be reduced by 28% with front-facing PV cells [6]. Other designs include cylinders [7], doped optical fibers [8,9], and cascaded primary and secondary luminescent plates [10].

Most recent work has attempted to incorporate quantum dots (QDs) as the fluorophore instead of dyes because the band gap of QDs can be tuned for specific applications and Pb-salt QDs in particular can have much wider absorption spectra than dyes [11–14]. Some research is focused on rare-earth materials, but their extremely limited absorption spectra has hampered their use [15–18]. The choice of matrix material is an important factor. One study found that nearly 80% of the QD's original fluorescence intensity in solvent was retained when incorporated into one polymer, while output was completely quenched in others [19]. Some have attempted to circumvent any losses upon incorporating in a matrix by fabricating an LSC device out of QDs in solution [20], though this is not a practical approach for a deployed system.

Cd-salt QDs have been the focus of much LSC research. Advanced synthesis techniques have led to investigations of type-II hetero-nanocrystals [21], doped QDs [22], nanorods [23], and other techniques to reduce self absorption, an important loss mechanism in LSCs. For the most efficient power generation, it is best to absorb as much of the sunlight as possible. However, Cd-salt QDs still suffer from a limited absorption spectrum, not much greater than the best single dye systems [24]. Coropceanu and Bawendi recently achieved state of the art optical efficiencies (η_{opt} = photons out/photons in) as high as 48% using CdSe/CdS core/shell QDs, for example, but only over a very narrow input spectral region, ~400–475 nm [25].

Pb-salt QDs are ideal from this perspective, having a wide absorption band across most or all of the visible spectrum. But, they suffered from very low quantum yields (QY) until recently, when "magic" sized Pb-salt QDs and others became available [26], having a QY high enough ($\geq$ 70%) to make them practical for use in LSCs. Previously, devices made from Pb-salt QDs had thus suffered from relatively low PCE compared to dye [27–29].

This work examines high QY PbSe QDs ($>$ 70%) in poly(lauryl methacrylate-co-ethylene glycol dimethacrylate) (P(LMA-co-EGDMA)) and Angstrom Bond, Inc. AB9093 epoxy. To the authors' knowledge, a P(LMA-co-EGDMA) matrix has not been reported for use with Pb-salt QDs—only rarely with Cd-salt QDs [11, 30]—and an AB9093 matrix has never been reported for LSC use. Additionally, a PCE of 4.74% is achieved with a geometric gain of 2 (defined as the ratio of collecting area, the top of the LSC, to the output area, two sides in this case), the best reported result for any QD LSC system under broad-band illumination (or calculated for solar illumination from the optical efficiency) and the best efficiency reported with a Si PV cell known to the authors.

2. Experimental

2.1. Nanocomposite LSC PV system fabrication

Numerous polymer systems were trialled as a part of this work, including titania and zirconia sol-gels, various poly(methyl methacrylate) preparations, and some two-part epoxies. Of these, P(LMA-co-EGDMA) and AB9093 showed the most promise for continued study.

QDs were synthesized with an estimated QY of 70% (before incorporation into polymer) as reported in Waldron et al. [31], based on the methods of Evans et al. [32]. They were then incorporated into the AB9093 or P(LMA-co-EGDMA) solution and cured in a glass and Teflon mold as described by Waldron et al. [31] under a nitrogen atmosphere. Two 0.15 mm thick glass cover slides were used to form the sides of the mold. AB9093 adheres to glass, so this became part of the LSC. P(LMA-co-EGDMA) does not adhere well to glass, so AB9093 was used to attach the cover slides after curing for ease of handling and mechanical protection of the LSC. The resulting device was 5.2 mm thick (4.9 mm of nanocomposite plus two glass cover slides). All samples were ground to size with 320 grit paper and finished with 600 grit paper on a Buehler polishing machine.

AB9093 was used as received from Fiber Optic Center, Inc. Lauryl methacrylate (96%, 500 ppm MEHQ inhibitor; LMA), ethylene glycol dimethacrylate (98%, 90–110 ppm MEHQ inhibitor; EGDMA), and bis(2,4,6-trimethylbenzoyl)-phenylphosphine oxide (97%; UV initiator) were used as received from Sigma-Aldrich. A stock solution of monomer was prepared by mixing $(80 \pm 0.5)\%$ LMA and $(20 \pm 0.5)\%$ EGDMA with $(0.1 \pm 0.025)\%$ UV initiator by weight under ambient atmosphere and degassing in a vacuum chamber. This ratio represents the result of trials to find a cured matrix with appropriate mechanical and optical properties, that is non-damaging to QD optical properties, and using the minimum quantity of initiator to fully cure the sample.

PV cells were attached to two opposite emitting edges of the LSC with AB9093 spot cured with a UV diode (QPhotonics, LLC UVTOP355). SunPower Corp. monocrystalline Si PV cells rated at 22% efficiency were used. The two edges not mated to a PV cell were coated with 3M$^{\text{TM}}$ Vikuiti Enhanced Specular Reflector (ESR) film (American Polarizers, Inc.), attached with 3M$^{\text{TM}}$ Optically Clear Adhesive 8142KCL film (Tekra). The ESR film is rated for reflectivity $> 98\%$ [33] and the adhesive film is rated for transmission $> 99\%$ [34].

2.2. I-V curve measurement

The broadband lamp measurement setup is shown in figure 1(a). A Thorlabs OSL1 fiber illuminator with a 150 W halogen lamp was used as a light source with a focal length $f = 25$ mm lens to provide even illumination. The LSC PV sample was held in place below the fiber tip and lens at a distance such that the average optical power incident on the LSC surface was 87.3 $\frac{\text{mW}}{\text{cm}^2}$. As seen in figure 1(b), this represents the power of the lamp required to provide a photon flux to the LSC equal to the photon flux of sunlight at Earth's surface with an energy greater than 1.1 eV [35] (1100 nm), the band gap of the Si PV cell used

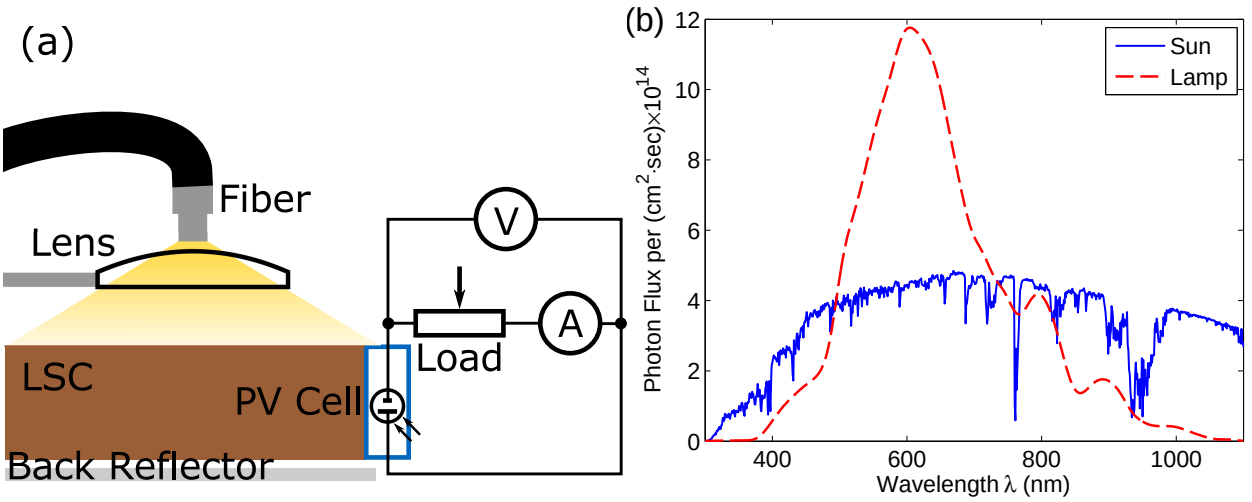

Figure 1: (a) Setup for measuring the I-V curve of the LSC PV system under broadband illumination. The LSC is placed below the fiber tip and lens, and the solar cell is attached to the measurement circuit consisting of a potentiometer, ammeter, and volt meter. A diffuse reflector is below the LSC. (b) Calculated solar [35] and measured lamp spectrum with equal photon flux below 1100 nm.

for testing. Thus, the number of photons that fall within the absorption spectral region of the QDs or PV cell will be the same under lamp illumination as under illumination by a standard ASTM air mass 1.5 solar spectrum, even though the spectra shape does not match exactly.

Optical power was measured with a Melles Griot 13PEM001 thermopile broadband power meter. A diffuse reflector with a Labsphere, Inc. Spectraflect® barium sulfate coating was placed below the sample with minimal separation.

A ten turn, 100 Ω, 2 W potentiometer and a Hewlett-Packard 3468A digital multimeter ammeter was connected to a single PV cell in series as the load, as shown in figure 1a. The minimum resistance through the potentiometer and ammeter load and all interconnects was ~0.5 Ω. A Fluke 8842A digital multimeter was connected in parallel across the load to measure voltage drop. The load was then varied to generate an I-V curve. MATLAB™ was used to fit a second order exponential curve to the data to find the maximum power point P_{mpp}, open circuit voltage V_{oc}, FF, and short circuit current I_{sc}.

2.3. Optical characterization

Optical absorption measurements were performed with a Beckman DU-650 absorption spectrophotometer. Data was recorded at 0.2 nm wavelength intervals with $\leq$ 1.8 nm spectral bandwidth. Measurements were referenced to clear samples, such as polymer samples without QDs. Steady-state fluorescence measurements were performed with a StellarNet EPP2000CXR-SR-200 spectrometer and recorded at 0.5 nm resolution. A 532 nm

wavelength doubled Nd-YAG laser was used as the excitation source. An absorbing long-pass filter was used to block the excitation wavelength from entering the spectrometer to prevent interference with the desired signal.

2.4. Temperature dependence

Samples were mounted in a convection oven over a diffuse reflector for electrical characterization at various temperatures. The samples were illuminated only when recording data by a Thorlabs OSL1 fiber illuminator through an opening in the top of the oven. A US Sensor PPG101A1 100 $\Omega \pm 0.06\%$ platinum resistance temperature detector (RTD) was attached to the sample mount with Arctic Silver Inc. Céramique thermal compound to provide an accurate temperature readout. V_{oc} and I_{sc} were then recorded using equipment detailed in section 2.2. A baseline measurement of a bare PV cell (PV cell without an LSC attached) was taken to correct for the PV cell temperature response.

3. Results and Discussion

Performance of the LSCs were rated on the basis of power conversion efficiency, PCE. PCE was computed in the standard way:

$$\mathrm{PCE} = \frac{P_{\mathrm{LSC}}}{P_{\mathrm{opt}}} = \frac{2 \cdot P_{\mathrm{mpp}}}{100\ \frac{\mathrm{mW}}{\mathrm{cm}^2} \cdot L_{\mathrm{LSC}} W_{\mathrm{LSC}}} \tag{1}$$

where P_{LSC} is the electrical power output from the LSC, P_{opt} is the optical power incident on the LSC, P_{mpp} is the measured electrical power from the PV cell at the maximum power point, and L_{LSC} and W_{LSC} are the length and width of the LSC top surface in cm. P_{LSC} is assumed to be twice P_{mpp} because PV cells are attached to two sides of the LSC but only one is measured.

The fill factor, FF, was also computed:

$$\mathrm{FF} = \frac{V_{\mathrm{mpp}} I_{\mathrm{mpp}}}{V_{\mathrm{oc}} I_{\mathrm{sc}}} \tag{2}$$

where V_{mpp} and I_{mpp} are the voltage and current at the maximum power point and V_{oc} and I_{sc} are the open circuit voltage and short circuit current.

To ensure proper operating conditions of the solar simulation setup, a PV cell matching the dimensions of the tested LSCs was measured and compared to specifications. The I_{sc} matched well, but the V_{oc} was low, indicating damage during preparation or substandard cells.

The best performing LSC was a P(LMA-co-EGDMA) sample with a QD concentration of 12.7 µM. The IV curve for this sample is shown in figure 2, and additional parameters are summarized in table 1. As expected, I_{sc} is lower than for the bare PV cell because the bare PV cell has twice the area of the PV cells attached to the LSC. The V_{oc} is also lower than

Table 1: Measured values for the Si PV cell and the most efficient P(LMA-co-EGDMA) QD LSC. PV cell values were measured under OSL1 lamp illumination. Specified values are NREL certified from literature [36] (shown in parenthesis) and manufacturer specified values for a module [37] (shown in square brackets). LSC values shown were measured under OSL1 and Solar Simulator lamp illumination.

		PV Cell		LSC	
		Measured	Specified	OSL1	Solar Sim.
V_{oc}	mV	600.0	(724.7)	544.0	560.3
I_{sc}	mA	169.6	(170.2)	27.60	26.53
V_{mpp}	mV	471.5	[569.8]	428.9	426.8
I_{mpp}	mA	152.6	[157.3]	24.02	23.2
FF	%	70.7	(80.1)	68.13	66.5
PCE	%	17.12	(22.4 ± 0.6)	4.93	4.74
length	cm	2.1	2.1	2.1	2.1
width	cm	2.1	2.1	2.0	2.0

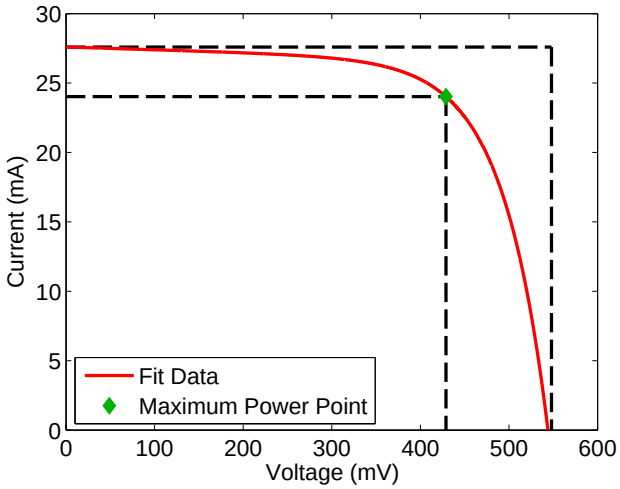

Figure 2: The I-V curve for the best performing LSC sample under OSL1 lamp illumination. The diamond is the maximum power point, and the dotted lines are guides for the eye for important current and voltage values.

the bare PV cell, indicating it is not operating at full efficiency when attached to the LSC because of the lower incident photon flux.

The absorption and emission curves for QDs in P(LMA-co-EGDMA) are shown in figure 3; the spectra does not change significantly from those when the QDs are dispersed in hexane (not shown). The characteristic 1-s absorption peak occurs at a wavelength of 763 nm and the emission peak at 856 nm. This points to one potential route to a better PCE: by synthesizing slightly larger QDs, the spectra could easily be red shifted 50–100 nm. This

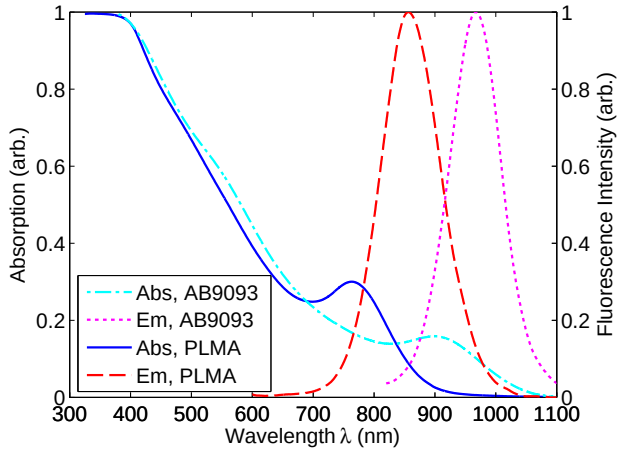

Figure 3: Optical absorption and emission of QDs in AB9093 epoxy and P(LMA-co-EGDMA).

would increase the amount of light absorbed by the sample without significantly dropping the external quantum efficiency of the solar cell at the peak fluorescence wavelength.

As shown in figure 3, the optical spectra of QDs in an AB9093 matrix is red shifted, as desired; this is due to an interaction between the QDs and the matrix, not a size change of the QDs. The absorption 1-s peak was at a wavelength of 898 nm and the fluorescence peak was at 968 nm. However, the AB9093 matrix adversely affects the QD fluorescent yield, causing the fluorescence to drop by about half [31]. Additionally, there is more opportunity for self absorption losses in AB9093 because the Stokes shift, the separation between the absorption of emission peak, was only 70 nm instead of 93 nm in P(LMA-co-EGDMA). QY in P(LMA-co-EGDMA) is nearly unaffected, enabling a higher PCE. The PCE of the PLMA samples was 71.1% higher, relatively, than the AB9093 samples.

The LSC PCE is expected to be highly dependent on QD concentration. The PCE will first rise sharply with increasing QD concentration as the LSC is able to absorb more of the incident light. As concentration continues to rise, PCE will reach a peak and then begin to fall as emitted photons are self-absorbed by other QDs and lost before reaching the PV cell. This drop is expected to occur more slowly than the initial rise.

To confirm this, two P(LMA-co-EGDMA) LSC samples with lower and higher concentrations of QDs were fabricated. Concentrations of 10.8 μM and 14.6 μM (ideal concentration ±15%) were used. The PCE of both samples was indeed lower, with the lower QD concentration sample showing a −18.4% fractional change and the higher concentration showing a −11.9% fractional change from the ideal concentration. As expected, the sample with a concentration lower than the ideal had a PCE lower than the sample with a concentration higher than the ideal. This trend was also seen in AB9093 samples. This time the concentration was varied by ±12.5% and the resultant fractional change in PCE was −21.3% and −6.1%.

In general, it is very difficult to measure these losses separately from one another because

of how much they interact; thus, a ray trace simulation is generally used to predict the relative strength of each loss for a given LSC configuration [38]. For example, increased scattering will increase self absorption, QY loss, and others, but decrease unabsorbed radiation. Besides self absorption, non-unity QY, and unabsorbed radiation discussed above, other loss mechanisms include total internal reflection (TIR) loss, front surface reflection (FSR), escape cone, matrix absorption, scattering, and mirror loss. Of these, only FSR can be accurately predicted analytically. The Fresnel equations can be used for this purpose; at normal incidence, FSR can be approximated using the refractive index n of the glass cladding:

$$\mathrm{FSR} \approx \left(\frac{1-n}{1+n}\right)^2. \tag{3}$$

Escape cone loss L_{EC} describes photons which are emitted from a luminophore inside of the solid angle cone formed by the critical angle θ_{c} within which total internal reflection will not occur. It can be calculated for a given n [39, 40]:

$$L_{\mathrm{EC}} = 1 - \cos\theta_{\mathrm{c}} = 1 - \frac{\sqrt{n^2-1}}{n}. \tag{4}$$

But this only gives a very rough idea of escape cone loss, as it does not account for the bottom reflector or the relative dominance of other loss events (e.g. a photon can be emitted within the loss cone, but be reabsorbed before it exits the matrix).

Other losses can also be estimated to an extent without resorting to simulations. Total internal reflection loss is the leakage of photons from the waveguide which would otherwise be propagated via TIR. Here, it is due primarily to surface imperfections, and is expected to be a few percent or less [41]. Mirror loss is the result of non-unity reflectivity of the side and bottom mirrors, and is typically a few percent or less when high quality mirrors are used.

Further confounding the interplay of losses is the fact that some scale with LSC size, whereas others do not. These "transport" losses which scale include matrix absorption, scattering, and TIR loss. Total transport loss in poly(methyl methacrylate) at $\lambda \approx 633$ has been estimated at ~1–3%/cm [41], but it will be higher in the near IR as a result of weak absorption bands of the polymer [31]. Self absorption also scales to an extent, but saturates over a relatively short distance: only photons in a certain spectral region can be lost to self absorption, and eventually these are all lost.

Previous work by the authors investigating the temperature dependent fluorescent properties of QDs similar to those used in this work suggested that there would be a decrease in LSC performance as the ambient temperature is increased [42]. An AB9093 and a P(LMA-co-EGDMA) LSC sample was fabricated and tested over a temperature range of ~20–40°C.

As expected, both I_{sc} (figure 4a) and V_{oc} (figure 4b) decreased with rising temperature, a result of decreased QD fluorescence. I_{sc} falls linearly with temperature because of the linear decrease in fluorescence intensity and optical absorption with temperature [42]. The P(LMA-co-EGDMA) LSC sample suffers less performance degradation with temperature, with the I_{sc} falling at $-0.58\%/^{\circ}\mathrm{C}$, relatively, compared to the AB9093 sample's $-0.75\%/^{\circ}\mathrm{C}$.

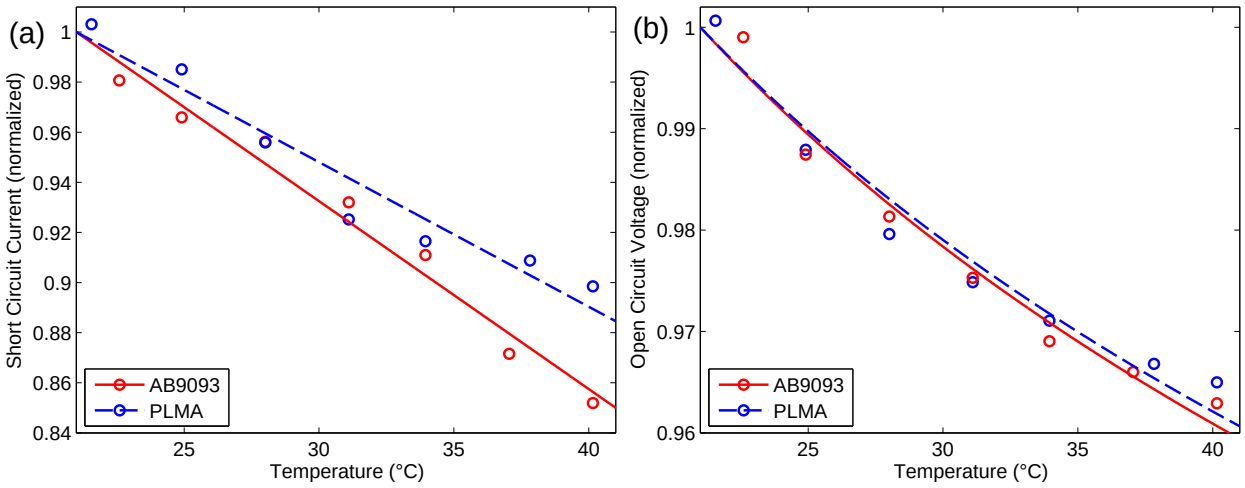

Figure 4: (a) Short circuit current with linear fit lines and (b) open circuit voltage with logarithmic fit lines of LSC samples as a function of temperature, corrected for PV cell response. Both fall with increasing temperature as a result of reduced QD fluorescence [42].

V_{oc} decreases logarithmically according to the relation [43]:

$$V_{oc} = \frac{k_B T}{e} \ln\left[\frac{I_{sc}}{I_0} + 1\right] \tag{5}$$

where k_B is Boltzmann's constant, T is absolute temperature, e is the elementary charge, and I_0 is the saturation current density. The change in V_{oc} shown in figure 4b was fit to an equation of the form $V_{oc} = a\ln(T) + b$ where a and b are fitting parameters. Both LSC types decline to about 96% of their 20°C value at 40°C with the P(LMA-co-EGDMA) sample again outperforming the AB9093 sample. These results suggest that increasing the ambient temperature from room temperature to 40°C will decrease the PCE of the best P(LMA-co-EGDMA) sample from 4.74% to ~4%.

4. Conclusion

Lead selenide QD LSCs were fabricated and their performance was measured with monocrystalline Si PV cells. The resulting LSC system had the highest measured PCE of any system making use of a Si PV cell, 4.74%. This is also the highest known broadband PCE of any system using QDs as the luminophore, calculated or measured. It also has a higher optical efficiency than the state of the art dye module, 0.26 verses 0.2, respectively (calculated from the PCE).

There are many routes forward to improve PCE. The most obvious improvement is a slight change to the QD size to alter its band gap. If the QD were made smaller (not a trivial task given their already small size, ~2.5 nm diameter), the LSC could potentially be matched to a GaAs cell. But, given the price of Si PV cells compared to GaAs PV cells, this

might not be a cost effective option. Alternately, the QDs could be made slightly larger to shift their emission closer to the band edge of Si. This would also shift the absorption curve by nearly the same amount, allowing a greater portion of the solar spectrum to be absorbed.

The QY could also be further improved. According to ray trace simulations performed by our group, if QDs with a QY of 90% were used, the resulting PCE would be ~7%. While this QY has been achieved for similar QDs in literature, consistency of production and incorporating them into polymer without damage remains an issue. Finally, ensuring high quality PV cells are appropriately mated would improve performance to a predicted ~5.7%. These cells were specified at 724.7 mV, but only 600.0 mV was measured. Either these were sub-standard PV cells, or they became damaged in some way during the fabrication process. In conjunction with a QY increase, the predicted PCE is ~8.5%.

References

[1] Weber W and Lambe J 1976 *App. Opt.* **15** 2299–300

[2] Goetzberger A and Greubel W 1977 *Appl. Phys.* **14** 123–39

[3] Slooff L, Bende E, Burgers A, Budel T, Pravettoni M, Kenny R, Dunlop E and Büchtemann A 2008 *Phys. Stat. Sol.* **2** 257–9

[4] Desmet L, Ras A, de Boer D and Debije M 2012 *Opt. Lett.* **37** 3087–89

[5] Peters M, Goldschmidt J, Löper P, Groß B, Üpping J, Dimroth F, Wehrspohn R and Bläsi B 2010 *Energies* **3** 171–93

[6] Corrado C, Leow S, Osborn M, Chan E, Balaban B and Carter S 2013 *Sol. Energ. Mat. Sol. Cells* **111** 74–81

[7] Wang T, Yu B, Chen B, Hu Z, Luo Y, Zou G and Zhang Q 2013 *J. Opt.* **15** 055709

[8] Banaei E and Abouraddy A 2013 *Prog. Photovolt. Res. Appl.*

[9] Edelenbosch O, Fisher M, Patrignani L, van Sark W and Chatten A 2013 *Opt. Lett.* **21** A503–14

[10] Daorta S, Proto A, Fusco R, Andreani L and Liscidini M 2014 *Appl. Phys. Lett.* **104** 153901

[11] Bomm J, Büchtemann A, Chatten A, Bose R, Farell D, Chan N, Xiao Y, Slooff L, Meyer T, Meyer A, van Sark W and Koole R 2011 *Sol. Energ. Mat. Sol. Cells* **95** 2087–94

[12] Krumer Z, Pera S, van Dijik-Moes R, Zhao Y, de Brouwer A, Groeneveld E, van Sark W, Schropp R and de Mello Donegá C 2013 *Sol. Energ. Mat. Sol. Cells* **111** 57–65

[13] Meinardi F, Colombo A, Velizhanin K, Simonutti R, Lorenzon M, Beverina L, Viswanatha R, Klimov V and Brovelli S 2014 *Nature Photon* **8** 392–9

[14] Reisfeld R 2010 *Opt. Mater.* **32** 850–6

[15] Liu C, Deng R, Gong Y, Zou C, Lui Y, Zhou X and Li B 2014 *Int. J. Photoenergy* **2014**

[16] Correia S, de Zea Bermudez V, Ribeiro S, André P, Ferreira R and Carlos L 2014 *J. Mater. Chem. A* **2** 5580–96

[17] Nolasco M, Vaz P, Freitas V, Lima P, André P, Ferreira R, Vaz P, Ribeiro-Claro P and Carlos L 2013 *J. Mater. Chem. A* **1** 7339–50

[18] Wang T, Zhang J, Ma W, Luo Y, Wang L, Hu Z, Wu W, Wang X, Zou G and Zhang Q 2011 *Solar Energy* **85** 2571–9

[19] Gallagher S, Rowan B, Doran J and Norton B 2006 *Solar Energy* **81** 540–7

[20] Sholin V, Olsin J and Carter S 2007 *J. Appl. Phys.* **101** 12114

[21] Krumer Z, Pera S, van Dijk-Moes R, Zhao Y, de Brouwer A, Groeneveld E, van Sark W, Schropp R and de Mello Donegá C 2013 *Sol. Energ. Mat. Sol. Cells* **111** 57–65

[22] Erickson C, Bradshaw L, Bradshaw S, McDowall S, Gilbertson J, Gamelin D and Patrick D 2014 *ACS Nano.* **8** 3461–7

[23] Bronstein N, Li L, Xu L, Yao Y, Ferry V, Alivisatos A and Nuzzo R 2013 *ASC Nano* **8** 44–53

[24] Purcell-Milton F and Gun'ko Y 2012 *J. Mater. Chem.* **22** 16687–97

[25] Coropceanu I and Bawendi M 2014 *Nano Lett.* **14** 4097–101

[26] Evans C, Guo L, Peterson J, Maccagnano-Zacher S and Krauss T 2008 *Nano Letters* **8** 2896–9

[27] Wang C, Shcherbatyuk G, Inman R, Pelka D,

Zhang W, Rodriguez Y, Carter S, Winston R and Ghosh S 2010 *Proc. of SPIE* **7772**

[28] Wilton S, Fetterman M, Low J, You G, Jiang Z and Xu J 2014 *Opt. Express* **22** A35–43

[29] Shcherbatyuk G, Inman R, Wang C, Winston R and Ghosh S 2010 *Appl. Phys. Lett.* **96** 191901

[30] Erickson C 2014 *Doped quantum dot luminescent solar concentrators* Masters thesis Western Washington University

[31] Waldron D, Preske A, Zawodny J, Krauss T and Gupta M 2015 *Nanotechnology* **26** 075705

[32] Evans C, Evans M and Krauss T 2010 *J. Am. Chem. Soc.* **132** 10973–75

[33] 3M Corp 2010 Vikuiti enhanced specular reflector (ESR) URL http://multimedia.3m.com/mws/media/374730O/vikuiti-tm-esr-sales-literature.pdf?fn=ESR%20ss2.pdf

[34] 3M Corp 2010 3M optically clear adhesive 8142KCL URL http://multimedia.3m.com/mws/media/7033940/3mtm-optically-clear-adhesive-8142kcl.pdf

[35] NREL Reference solar spectral irradiance: ASTM G-173 URL http://rredc.nrel.gov/solar/spectra/am1.5/ASTMG173/ASTMG173.html

[36] Green M A, Emery K, Hishikawa Y, Warta W and Dunlop E D 2015 *Prog. Photovolt: Res. Appl.* **23** 1–9

[37] Sunpower Corporation E19/ 320 solar panel URL http://us.sunpower.com/sites/sunpower/files/media-library/data-sheets/ds-e19-series-320-solar-panel-datasheet.pdf

[38] Waldron D 2015 *Lead selenide quantum dot luminescent solar concentrators* Phd thesis University of Virginia

[39] Shurcliff W and Jones R 1949 *J. Opt. Soc. Am.* **39** 912–6

[40] Keil G 1970 *Nuclear Instruments and Methods* **87** 111–23

[41] Thomas W, Drake J and Lesiecki M 1983 *Appl. Opt.* **22** 3440–50

[42] Waldron D, Preske A, Zawodny J, Krauss T and Gupta M *manuscript under review: Temperature dependent optical properties of lead selenide quantum dot polymer nanocomposites*

[43] Goetzberger A, Knobloch J and Voss B 1998 *Crystalline Silicon Solar Cells* (John Wiley & Sons, Ltd)